type of junction. It is further demonstrated that the Wu and Rosenbaum tracking circulator belongs to this type of device. The agreement between the closed form expression for the loaded Q-factor of the junction and a numerical calculation are in excellent agreement.

ACKNOWLEDGMENT

The author would like to thank Hugh Conner of Heriot-Watt University for the computations in this paper.

REFERENCES

[1] J. W. Simon, "Broadband strip-transmission line Y-junction circulators," *IEEE Trans. Microwave Theory Tech.*, vol. MTT-13, 335–345, May 1965.
[2] Y. S. Wu and F. J. Rosenbaum, "Wideband operation of microstrip circulators," *IEEE Trans. Microwave Theory Tech.*, vol. MTT-22, pp. 849–856, Oct. 1974.
[3] J. de Koning *et al.*, "Full band low loss continuous tracking circulation in K band," *IEEE Trans. Microwave Theory Tech.*, vol. MTT-25, pp. 152–157, Feb. 1977.
[4] J. Helszajn *et al.*, "Synthesis of stripline circulator using frequency independent real gyrators," *MOA*, to be published.
[5] S. Ayter and Y. Ayasi, "The frequency behaviour of stripline circulator junctions," *IEEE Trans. Microwave Theory Tech.*, vol. MTT-26, pp. 197–202, Mar., 1978.
[6] H. Bosma, "On stripline Y-circulation at UHF," *IEEE Trans. Microwave Theory Tech.*, vol. MTT-12, pp. 61–72, Jan. 1964.
[7] C. E. Fay and R. L. Comstock, "Operation of the ferrite junction circulator," *IEEE Trans. Microwave Theory Tech.*, vol. MTT-13, pp. 15–21, Jan. 1965.
[8] J. B. Davies and P. Cohen, "Theoretical design of symmetrical junction stripline circulators," *IEEE Trans. Microwave Theory Tech.*, vol. MTT-11, pp. 506–512, Nov. 1963.
[9] J. Helszajn, "The synthesis of quarter-wave coupled circulators with Chebyshev characteristics," *IEEE Trans. Microwave Theory Tech.*, vol. MTT-20, pp. 764–769, Nov. 1972.
[10] J. Helszajn, *Nonreciprocal Microwave Junctions and Circulators.* New York: Wiley, 1975.
[11] H. Bosma, "Junction Circulators," *Advances in Microwaves*, vol. 6, pp. 191–194, 219–223, 1971.

Propagation Constant Below Cutoff Frequency in a Circular Waveguide with Conducting Medium

TAKEO ABE, MEMBER, IEEE, AND YOSHIO YAMAGUCHI

***Abstract*—Exact and approximate propagation characteristics of normal modes in the cutoff region of a circular waveguide surrounded by a medium of finite conductivity are discussed. An exact solution is obtained by numerical analysis, and an approximate one is derived by expanding the characteristic equation considering the finite conductivity of the cylinder wall. The computed values are compared with experimental ones. It is shown that the attenuation of TM_{01} mode at frequencies that are much lower than the cutoff frequency is constant, i.e., independent of frequency and the material constants of the external medium, and this mode is the most suitable one for realizing a precision circular piston attenuator.**

I. INTRODUCTION

AT PRESENT, the dominant HE_{11} mode is used for circular piston attenuators operating below cutoff frequency. An approximate propagation theory [1], [2], has been derived for these attenuators under the assumption that the conductivity of the cylinder wall is infinite. The attenuation of the HE_{11} mode, by this theory, should be constant at frequencies that are much lower than the cutoff frequency. Experimental attenuation values, however, vary with frequency. This phenomenon seems to be caused by the finite conductivity of the guide wall. A correction to the attenuation of the HE_{11} mode has been reported by Brown [3].

Obviously, if a mode could be found that is independent of frequency and conductivity, an ideal attenuator could be realized based on this mode. For these reasons, we investigated several modes of circular waveguide, taking into consideration the finite conductivity of the guide wall.

This paper reports the propagation characteristics of normal modes in the cutoff region of a circular waveguide surrounded by a medium of finite conductivity. Exact and approximate propagation constants are derived, experimental values are presented, the distribution of E_z in the radial direction is discussed, and the ideal mode for a precision circular piston attenuator is pointed out.

II. CHARACTERISTIC EQUATION

A hollow circular cylinder of radius a and of infinite length is surrounded by a dissipative medium as shown in Fig. 1. No restriction is imposed on the conductivity of the external medium. The normal modes in this cylinder are of four types; circularly symmetric TE_{0m}, TM_{0m}, and hybrid HE_{nm}, EH_{nm} modes which reduce to TE_{nm}, TM_{nm} when the conductivity of the external medium becomes infinite. These modes are assumed to have time and z variation of

Manuscript received October 24, 1980; revised December 10, 1980.
The authors are with the Faculty of Engineering, Niigata University, Niigata, 950-21 Japan.

0018-9480/81/0700-0707$00.75 ©1981 IEEE

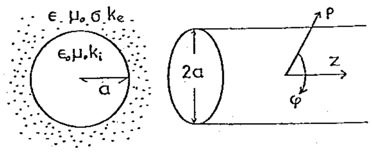

Fig. 1. Geometry of a circular waveguide and circular coordinate system (ρ, ψ, z).

the form $e^{j(\omega t - hz)}$, where h is the propagation constant. The propagation constants of normal modes in this cylinder must satisfy the characteristic equation which is given by Stratton [4]

$$\left(\frac{J_n'(u)}{uJ_n(u)} - \frac{H_n'(v)}{vH_n(v)}\right)\left(\frac{k_i^2 J_n'(u)}{uJ_n(u)} - \frac{k_e^2 H_n'(v)}{vH_n(v)}\right) = n^2h^2\left(\frac{1}{u^2} - \frac{1}{v^2}\right)^2 \quad (1)$$

where

$$u = \sqrt{k_i^2 - h^2}a \qquad v = \sqrt{k_e^2 - h^2}a$$
$$k_i^2 = \omega^2\epsilon_0\mu_0 \qquad k_e^2 = \omega^2\epsilon\mu_0 - j\omega\mu_0\sigma$$
$$h = \beta - j\alpha$$

- a radius,
- ω angular frequency,
- ϵ permittivity,
- μ_0 permeability,
- σ conductivity,
- β phase constant,
- α attenuation constant,
- $\epsilon_r = \epsilon/\epsilon_0$ relative dielectric constant,
- $J_n(u)$ Bessel function of order n,
- $H_n(v)$ Hankel function of the second kind of order n.

Primes denote differentiation with respect to the indicated argument throughout the paper.

It is difficult to obtain the exact solution of the propagation constant from (1) analytically, but it can be done by numerical analysis [5], [6].

III. Approximate Solution

When the conductivity of the external medium is in finite, the propagation constant is determined by the boundary condition that the electric field vanishes at the wall. It is well known that in this case the propagation constant in the cutoff region becomes purely imaginary and is given by

$$h = -j\alpha = -j(2\pi/\lambda_c)\sqrt{1-(\lambda_c/\lambda)^2}$$

where λ_c is cutoff wavelength and λ is wavelength of free space. But this propagation constant seems invalid for finite conductivity and for frequencies well below the cutoff frequency, because experimental attenuation values vary as the frequency decreases. Therefore, in order to find better approximate values for the propagation constant considering the effect of finite conductivity, we assume that, first, the conductivity is large but finite (i.e., $\omega\epsilon \ll \sigma$), and second, the radius a is greater than the skin depth δ ($\delta \ll a$).

The argument v and the ratio of Hankel functions can then be written in the following form:

$$v \cong k_e a \cong \sqrt{-j\omega\mu_0\sigma}\, a \cong (1-j)a/\delta$$
$$\frac{H_n'(v)}{H_n(v)} \cong \frac{n}{v} + \frac{H_{n+1}(v)}{H_n(v)} \cong \frac{n}{v} - j \cong -j. \quad (2)$$

Substituting (2) into (1), and neglecting terms of order lower than $O(v)^{-2}$, we get

$$\left(\frac{J_n'(u)}{uJ_n(u)} + j\frac{1}{v}\right)\left(\frac{k_i^2J_n'(u)}{uJ_n(u)} + j\frac{k_e^2}{v}\right) = n^2h^2\frac{1}{u^4}. \quad (3)$$

The propagation constant is seen to depend on the material constants of the external medium. We will examine the propagation characteristics of the HE and EH modes, and their dependence on the material constants.

A. HE_{nm} Mode

When the conductivity of the external medium is infinite, the propagation constant is determined by the root u_{nm} of

$$J_n'(u_{nm}) = 0. \quad (4)$$

For the case of finite conductivity, the root can be expressed as

$$u = u_{nm} + \Delta u \quad (5)$$

where Δu is a perturbation term. Taylor expansion of the Bessel function around the root u_{nm} leads to

$$J_n'(u) = J_n'(u_{nm} + \Delta u) \cong J_n''(u_{nm})\Delta u \cong \left(\frac{n^2}{u_{nm}^2} - 1\right)J_n(u_{nm})\Delta u$$
$$J_n(u) \cong J_n(u_{nm}). \quad (6)$$

Substituting (6) into (3) and neglecting terms of order higher than $O(\Delta u)^2$, Δu is given by

$$\Delta u = \frac{n^2(k_i^2a^2 - u_{nm}^2) + u_{nm}^4}{(n^2 - u_{nm}^2)(-ju_{nm}v)} \quad (7)$$

where $|k_i| \gg |k_e|$ is used.

Then the following approximate propagation constant can be derived:

$$h^2 \cong k_i^2 - (u_{nm}^2 + 2u_{nm}\Delta u)/a^2 \quad (8)$$

which for the cutoff region becomes

$$\alpha_{cnm} \cong A(1 + C/2) \quad (9)$$
$$\beta_{cnm} \cong -AC/2 \quad (10)$$

and for the propagation region is

$$\alpha_{pnm} \cong (BC/2)(1 - C/2) \cong BC/2 \quad (11)$$
$$\beta_{pnm} \cong B(1 + C/2) \quad (12)$$

where

$$A = 2\pi f_{nm}\sqrt{\epsilon_0\mu_0}\sqrt{1-(f/f_{nm})^2}$$

$$B = 2\pi f_{nm}\sqrt{\epsilon_0\mu_0}\sqrt{(f/f_{nm})^2 - 1}$$

$$C = \frac{\delta}{a}\,\frac{1 - \left(\dfrac{f}{f_{nm}}\right)^2 \dfrac{n^2}{n^2 - u_{nm}^2}}{(f/f_{nm})^2 - 1}$$

and f_{nm} is the cutoff frequency. The propagation constant for the TE_{0m} mode is found from these equations by setting $n=0$.

For the dominant HE_{11} mode, which is presently used for piston attenuators, the following propagation constant in the cutoff region is found from (9) and (10):

$$\alpha_{c11} = \frac{15.99}{a}\sqrt{1 - \left(\frac{f}{f_{11}}\right)^2}\left[1 - \frac{\delta}{2a}\,\frac{1 + (f/f_{11})^2/2.391}{1 - (f/f_{11})^2}\right]$$

$$\cong \frac{15.99}{a}\left(1 - \frac{\delta}{2a}\right) \quad (\mathrm{dB/m}) \tag{13}$$

$$\beta_{c11} \cong \frac{1.842}{a}\,\frac{\delta}{2a}\,\frac{1 + (f/f_{11})^2/2.391}{\sqrt{1 - (f/f_{11})^2}} \quad (\mathrm{rad/m}). \tag{14}$$

B. EH_{nm} Mode

The EH_{nm} mode is characterized by the root u_{nm} of

$$J_n(u_{nm}) = 0. \tag{15}$$

In a similar manner as before, the propagation constant becomes for the cutoff region

$$\alpha_{cnm} \cong A(1 + D/2) \tag{16}$$

$$\beta_{cnm} \cong -(AD/2)(1 - D/2) \tag{17}$$

and for the propagation region

$$\alpha_{pnm} \cong (BD/2)(1 - D/2) \cong BD/2 \tag{18}$$

$$\beta_{pnm} \cong B(1 + D/2) \tag{19}$$

where

$$D = \frac{\delta}{a}\,\frac{(f/f_{nm})^2}{(f/f_{nm})^2 - 1}.$$

When putting $n=0$ in these equations, they correspond to the TM_{01} modes. From this, the propagation constant for the lowest order TM_{01} mode in the cutoff region becomes

$$\alpha_{c01} = \frac{20.9}{a}\sqrt{1 - \left(\frac{f}{f_{01}}\right)^2}\left[1 - \frac{\delta}{2a}\,\frac{(f/f_{01})^2}{1 - (f/f_{01})^2}\right] \quad (\mathrm{dB/m}) \tag{20}$$

$$\cong \frac{20.9}{a} \quad (f \ll f_{01}) \quad [\mathrm{dB/m}] \tag{21}$$

$$\beta_{c01} = \frac{2.405}{a}\cdot\frac{(\delta/a)(f/f_{01})^2}{2\sqrt{1 - (f/f_{01})^2}}\left[1 + \frac{\delta}{2a}\,\frac{(f/f_{01})^2}{1 - (f/f_{01})^2}\right] \quad (\mathrm{rad/m}). \tag{22}$$

Equations (11), (12), (18), (19), derived for the propagation region, are identical to those obtained by a perturbation method well known in waveguide theory [7].

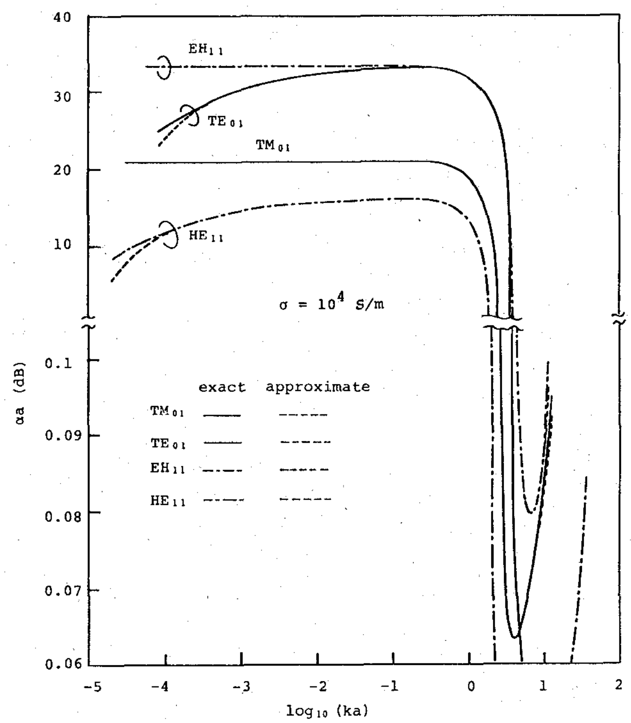

Fig. 2. Attenuation for each mode.

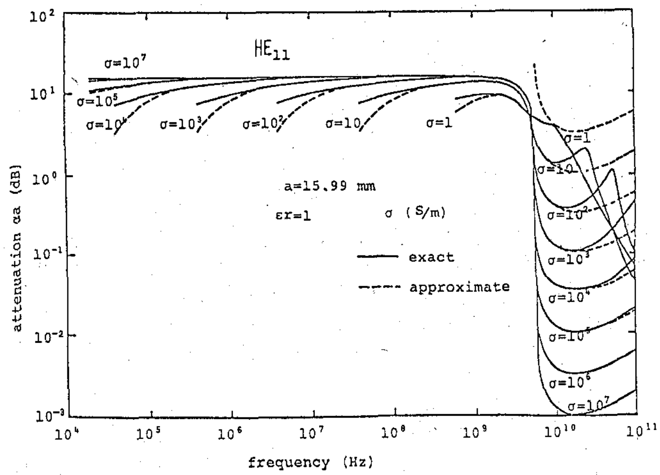

Fig. 3. Frequency characteristics of attenuation (HE_{11} mode).

IV. Numerical Results

Exact propagation constants can be obtained by solving (1) numerically. Equation (1) can be written in the form

$$F(u) = 0. \tag{23}$$

The algorithm used for solving (23) is based on Newton's method. The convergence conditions imposed on the relative error were 10^{-6} in magnitude, and 10^{-5} on the imaginary part.

As a numerical example, the attenuation for the lowest order modes HE_{11}, EH_{11}, TE_{01}, and TM_{01}, and a comparison between exact and approximate solutions are shown in Fig. 2 as a function of the normalized circumference ka and for a conductivity of 10^4 S/m. It is found that the approximate solutions are in good agreement with the exact ones.

Fig. 3 shows how the attenuation depends on the con-

TABLE I
FREQUENCY CHARACTERISTICS OF ATTENUATION (TM_{01} MODE)

σ (S/m)	ATTENUATION (dB) αa											
	εr=10						εr=1					
	10^0		10^4		10^7		10^0		10^4		10^7	
f (MHz)	exact	app.	exact	app.	exact	app.	exact	app.	exact	app.	exact	app.
6000	11.6495	6.0833	11.4221	11.4222	11.4744	11.4744	9.1688	6.0833	11.4211	11.4222	11.4744	11.4744
2000	19.5313	19.4678	20.0556	20.0556	20.0613	20.0613	19.0546	19.4678	20.0556	20.0556	20.0613	20.0613
1000	20.2860	20.4809	20.6825	20.6825	20.6844	20.6844	20.2094	20.4809	20.6825	20.6825	20.6844	20.6844
600	20.5482	20.7210	20.8141	20.8141	20.8150	20.8150	20.5353	20.7210	20.8141	20.8141	20.8150	20.8150
200	20.7541	20.8619	20.8798	20.8798	20.8799	20.8799	20.7881	20.8619	20.8798	20.8798	20.8799	20.8799
100	20.8399	20.8797	20.8860	20.8860	20.8860	20.8860	20.8402	20.8797	20.8860	20.8860	20.8860	20.8860
60	20.8597	20.8844	20.8873	20.8873	20.8873	20.8873	20.8599	20.8844	20.8873	20.8873	20.8873	20.8873
20	20.8788	20.8874	20.8880	20.8880	20.8880	20.8880	20.8788	20.8874	20.8880	20.8880	20.8880	20.8880
10	20.8835	20.8878	20.8880	20.8880	20.8880	20.8880	20.8835	20.8878	20.8880	20.8880	20.8880	20.8880
6	20.8853	20.8880	20.8880	20.8880	20.8880	20.8880	20.8853	20.8880	20.8880	20.8880	20.8880	20.8880
2	20.8871	20.8880	20.8880	20.8880	20.8880	20.8880	20.8871	20.8880	20.8880	20.8880	20.8880	20.8880
1	20.8876	20.8880	20.8880	20.8880	20.8880	20.8880	20.8876	20.8880	20.8880	20.8880	20.8880	20.8880
0.6	20.8878	20.8880	20.8880	20.8880	20.8880	20.8880	20.8878	20.8880	20.8880	20.8880	20.8880	20.8880
0.2	20.8880	20.8880	20.8880	20.8880	20.8880	20.8880	20.8880	20.8880	20.8880	20.8880	20.8880	20.8880

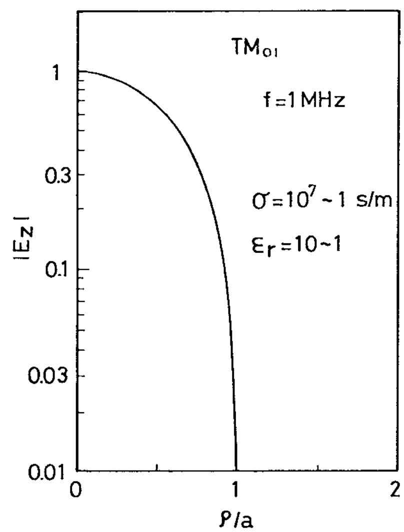

Fig. 4. z-component of electric field in radial direction.

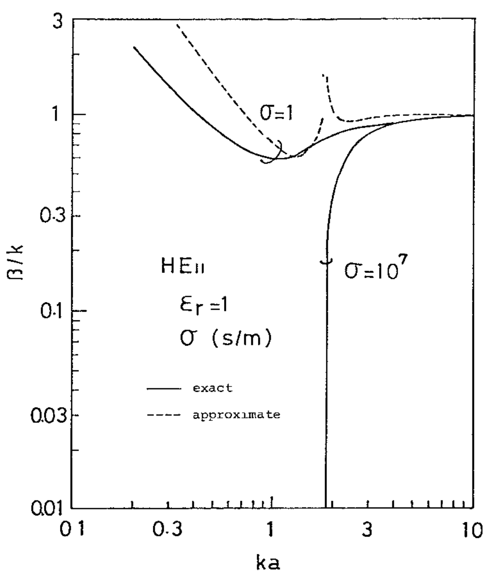

Fig. 5. Dispersion relation of HE_{11} mode.

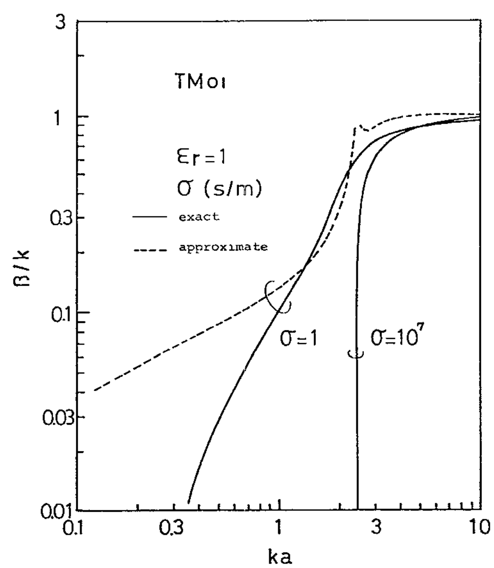

Fig 6. Dispersion relation of TM_{01} mode.

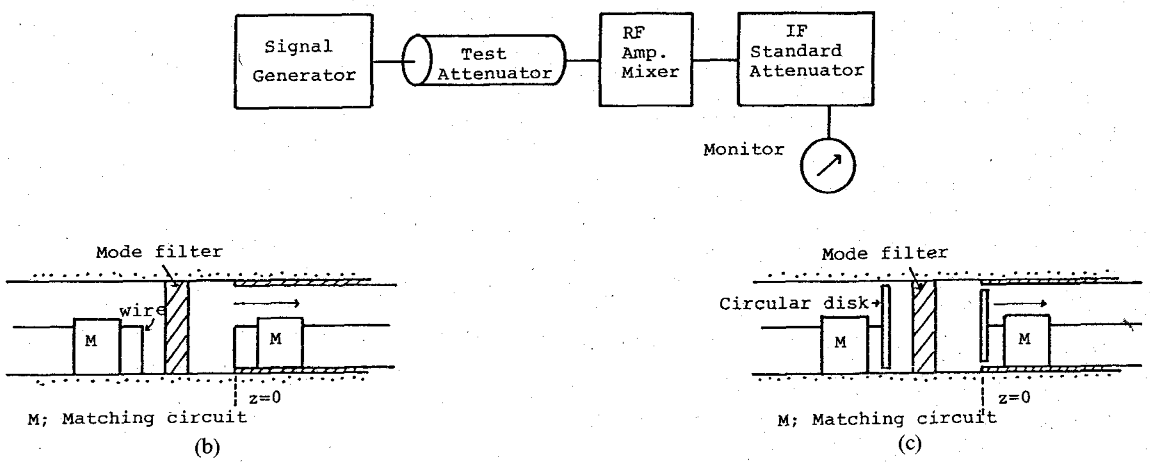

Fig. 7. Measurement apparatus. (a) Block diagram. (b) Side view of the test attenuator of HE_{11} mode. (c) Side view of the test attenuator for TM_{01} mode.

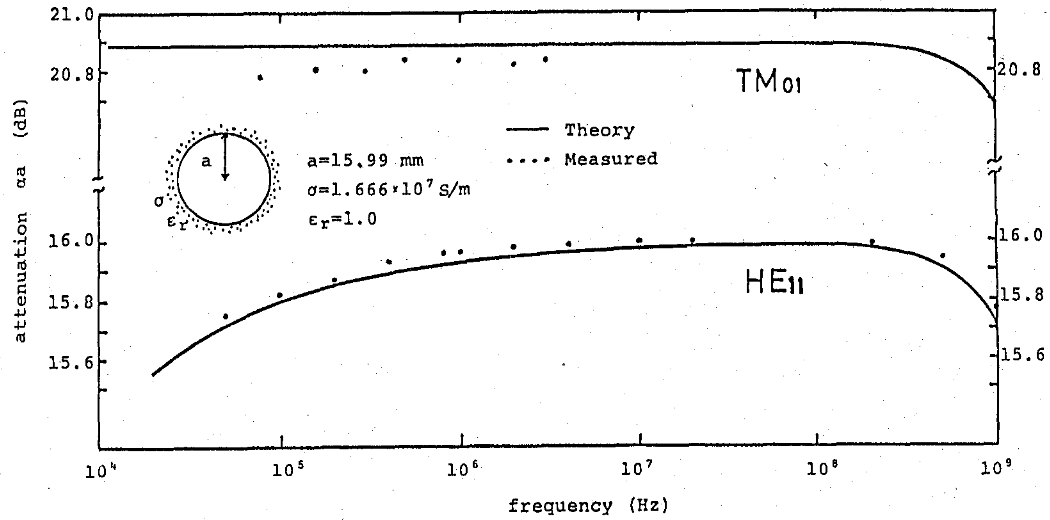

Fig. 8. Experimental and theoretical attenuation.

ductivity for the HE_{11} mode. It is seen that the approximate solution in this case agrees well with the exact one in the cutoff region when the conductivity is over 10^2 S/m. But the attenuation varies with frequency, and an error between exact and approximate solution appears as the frequency becomes lower. The reason for this error is that the second assumption $a \gg \delta$ is not satisfied anymore and a skin effect occurs. A similar error occurs in the propagation region when the conductivity is less than 10^4 S/m. The first assumption $\sigma \gg \omega\epsilon$ is violated in this case.

It should be noted in Table I that the attenuation of the TM_{01} mode is constant, i.e., independent of conductivity and frequency. This phenomenon can be explained by observing that the $(f/f_{01})^2$ term in the approximate equation (20) is superior to the δ/a term. The effect can also be explained phenomenologically from the exact solution, because it is seen that the z-component of the electric field, shown as a function of ρ/a in Fig. 4, does not change as a function of ϵ_r and σ and $E_z \cong 0$ for $\rho = a$.

Phase constants of the HE_{11} and TM_{01} modes, as a numerical example, are shown in Figs. 5 and 6. The approximate phase constants in the cutoff region do not agree with the exact ones for small conductivities less than 10^7 S/m. The phase constant, however, does not seem to have a significant meaning in the cutoff region.

V. Experimental Values

In order to confirm the theoretical results, we measured the attenuation of the HE_{11} and TM_{01} modes in the cutoff region. The measurement apparatus is shown in Fig. 7. We used a mode filter to suppress the undesired modes and used circular disks for the TM_{01} mode and wires or coils for the HE_{11} mode as the exciting and receiving antennas, in order to get the desired mode.

The test attenuator used was a hollow pipe made of brass with a conductivity of 1.666×10^7 S/m. The size of the pipe was about 30 cm long with a radius of 15.99 mm. As attenuation is a function of the length between the exciting and the receiving antennas, we obtained the attenuation of each mode by moving the receiving antenna about 0–6 cm.

Fig. 8 shows good agreement between experimental and theoretical values; the approximate values, incidentally, coincide with the exact ones.

VI. Conclusion

It is shown that, first, approximate propagation constants of circular waveguide modes agree well with exact ones when the conductivity of the waveguide wall is large ($\sigma \gg \omega\epsilon$) and the skin depth is smaller than the radius of the cylinder; second, that the attenuation of the TM_{01} mode is constant, i.e., independent of the material constants of the external medium and frequencies that are much lower than the cutoff frequency. The second result turns out to make the TM_{01} mode the most suitable for circular precision attenuators in the region where the attenuation of the dominant HE_{11} mode varies with frequency.

References

[1] E. G. Linder, "Attenuation of electromagnetic field in pipes smaller than critical size," *Proc. Inst. Radio Eng.*, vol. 30, pp. 554–556, Dec. 1942.
[2] A. L. Cullen, "Waveguide field pattern in evanecent modes," *Wireless Eng.*, vol. 26, pp. 317–322, Oct. 1949.
[3] J. Brown, "Correction to the attenuation constants of piston attenuators," *Proc. Inst. Elec. Eng.*, vol. 96, pp. 491–495, pt. 3, 1949.
[4] J. A. Stratton, *Electromagnetic Theory*. New York: McGraw-Hill, 1941, ch. 9, p. 526.
[5] J. I. Glaser, "Attenuation and guidance of modes on hollow dielectric waveguides," *IEEE Trans. Microwave Theory Tech.*, vol. MTT-17, pp. 173–174, Mar. 1969.
[6] Y. Yamaguchi and T. Sekiguchi, "Propagation characteristics of normal modes in hollow circular cylinder surrounded by dissipative medium," *Trans. IECE of Japan*, vol. 62-B, no. 4, pp. 368–373, Apr. 1979 (in Japanese).
[7] V. M. Papadopoulos, "Propagation of electromagnetic waves in cylinderical waveguides and imperfectly conducting walls," *Quart. J. Mech. Appl. Math.*, vol. 7, pp. 325–334, Sept. 1954.

Scattering of the TE_{01} and TM_{01} Modes on Transverse Discontinuities in a Rod Dielectric Waveguide—Application to the Dielectric Resonators

PHILIPPE GELIN, SERGE TOUTAIN, PATRICK KENNIS, AND JACQUES CITERNE

***Abstract*—Our purpose is to determine the resonance frequency together with the radiation quality factor of dielectric resonators. To do that, the reflection and the scattering properties of the TE_{01} and TM_{01} modes, incident on an abruptly ended dielectric rod, are analyzed. After the building of the complete mode spectrum on each side of the discontinuity, the continuity relations in the discontinuity plane associated with the orthogonality properties lead to a coupled integral equation system. That one is solved by means of an iterative procedure, providing all the characteristics of the discontinuity (reflection or coupling coefficients, radiation losses). Then, these solutions are used to determine the resonant frequency and the radiation quality factor of cylindrical resonators which are considered as waveguide lengths between two interacting discontinuities.**

Manuscript received October 13, 1980; revised February 3, 1981.
The authors are with the Centre Hyperfréquences et Semiconducteurs, L. A. au C. N. R. S. no. 287, Université des Sciences et Techniques de Lille, 59655 Villeneuve D'Ascq Cedex, France.

I. Introduction

IN THE LAST FEW YEARS, the availability of dielectric materials with high relative permittivity has given a great impact on the use of dielectric resonators in microwave integrated circuits (passband filters, stabilized solid-state sources).

The concept of dielectric resonator has been proposed in [1] as far back as 1939. The first analysis of the magnetic dipole resonance of cylindrical dielectric resonators of very high permittivity was treated under the assumption that all